JOURNAL OF MATERIALS SCIENCE **40** (2005) 861–870

Roughening transition of grain boundaries in metals and oxides

D. Y. YOON, Y. K. CHO
Department of Materials Science & Engineering, Korea Advanced Institute of Science and Technology, Taejon 305-701, Korea
E-mail: dyyoon@kaist.ac.kr

Extensive theoretical analysis and experimental observations show surface roughening transitions of crystals. The surface roughening is characterized by step free energy, which gradually decreases to 0 at the roughening transition temperature. For a crystal of finite size, the surface roughening transition is manifested by gradual increase of the curved edge and corner areas. In alloys, the interfaces between the solid and the liquid phases can be either singular, partially rough, or completely rough at different temperatures. Their thermally induced roughening transitions are similar to those of the solid-vapor interfaces. The interface roughening and the reverse transition to singular structures can also be induced by additives. The grain boundaries of any misorientation angles in oxides and metals also show roughening transitions. The singular grain boundaries have either flat, hill-and-valley, or kinked shapes, and with temperature increase or composition changes, they become defaceted to curved shapes. These defaceted grain boundaries are rough. It is thus possible to produce either singular or rough grain boundaries by heat-treatment or additives to vary their properties. © *2005 Springer Science + Business Media, Inc.*

1. Introduction

Structure and properties of a grain boundary depend on the direction of the grain boundary plane as well as the misorientation angle between the grain pair. If grain growth is relatively slow in a bulk polycrystal, the positions and normal directions of the grain boundaries will be determined by the condition to locally minimize the total grain boundary energy. The minimum grain boundary energy configuration is in turn determined by the variation of the grain boundary energy with its normal, which is usually represented by the polar plot of the grain boundary energy γ_g against the grain boundary normal n or the grain boundary Wulff plot $\gamma_g(n)$. The $\gamma_g(n)$ plot will depend on the misorientation angle between a pair of grains and will determine the equilibrium shape of a grain embedded in another grain with the particular misorientation angle. Although such island grains can be produced, their equilibrium shapes are difficult to observe because they tend to shrink and disappear rapidly during heat-treatment. But at least conceptually it is useful to consider such grain boundary Wulff shapes, and often stable segments of grain boundaries can represent a part of such a Wulff shape.

Like surfaces, there can be cusps in a $\gamma_g(n)$ plot, corresponding to flat grain boundary segments. When there are cusps in a $\gamma_g(n)$ plot, the grain boundary of an arbitrary average orientation is likely to have a hill-and-valley (h&v) structure, as explained by Herring [1]. With temperature increase or composition change, a cusp in a $\gamma_g(n)$ plot may disappear when the flat boundary segment becomes rough. If a grain boundary has an h&v structure, it will become defaceted with a curved shape. Usually, the defaceting transition is thus a manifestation of the grain boundary roughening transition.

Analogous surface roughening transition has been extensively studied theoretically [2–9] and experimentally [5–9]. The possibility of roughening transition of a symmetric grain boundary in Cu was proposed by Rottman [10] on the basis of estimated grain boundary step energy. Grain boundary faceting and defaceting transitions with either temperature change or additives have been observed in a number of metallic (Al [11], Cu-Bi [12], Fe-Te [13], Ni [14, 15], Ag [16]) and oxide (alumina [17, 18], $BaTiO_3$ [19–22]) systems. In alumina doped with SiO_2 and CaO [18] and in TiO_2-excess $BaTiO_3$ [23, 24], the grain boundaries running straight across the triple junctions were identified as the singular boundaries, and they were observed to become curved and hence rough with additives. These grain boundary transitions were observed for grain boundaries of any misorientation angles between the grain pairs.

In addition to grain boundary shape changes, there have been additional indirect evidences for grain boundary transitions in the temperature dependence of grain boundary energy [25], sliding [26–28], and migration [29–31]. In many metals and oxides [15–22], abnormal and normal grain growth behaviors were observed to be correlated with grain boundary roughening. Other mechanical, chemical, and electrical properties are also expected to depend on the roughening transition. Therefore, it will be important in grain boundary engineering.

In this report, the grain boundary roughening transitions in metals and two oxides will be reviewed. First, the analogous surface roughening transition, which has been more completely studied, will be examined, followed by a discussion of the relationship between the roughening and defaceting transitions. The grain boundary roughening transitions in metals and oxides will then be discussed in separate sections. And finally, the kinetics of the grain boundary roughening transition and metastable boundary structures will be examined and related to properties. Almost all examples of grain boundaries presented in this report will be drawn from either pure or single phase systems.

2. Surface roughening transition

The surface roughening was first proposed by Burton, Cabrera, and Frank [2–4] based on Onsager's solution of the two dimensional Ising model [32], which predicted a second order transition. The later theories and experiments of surface roughening transition have been reviewed by Weeks and Gilmer [5], Weeks [6], Beijern and Nolden [7], Wortis [8], and Conrad [9]. The solutions of the solid-on-solid (SOS) or the equivalent models predicted an infinite order surface roughening transition [33–36], which can be represented by step free energy $\sigma(T)$ gradually decreasing to 0 at the roughening temperature. If the value of $\sigma(T)$ is larger than 0, the surface is singular with a flat shape, corresponding to a cusp in the Wulff plot of the surface energy $\gamma(n)$. A rough surface with $\sigma(T)$ equal to 0 will have a curved shape without any cusp in the $\gamma(n)$ plot. Thus, the roughening transition is manifested in the surface shape change. Rottman and Wortis [37] predicted with a lattice gas model that the edges and corners of cubic crystals would become curved as temperature increases with the size of the flat surface decreasing linearly with $\sigma(T)$ until both became 0 at the roughening transition temperature T_R.

The surface movement also depends on its structure. A singular surface free of defects is predicted to grow by two dimensional nucleation of steps [2–5], while a rough surface will grow continuously without any step nucleation. Thus, the growth rate of a singular surface will show an exponential dependence on supersaturation, while a rough surface will grow linearly with supersaturation. The step fluctuation at surface is also predicted to show a critical behavior at and above T_R.

Extensive experiments have been performed on ^{4}He crystals in order to test some of these theoretical predictions [38–41] by taking advantage of superfluid matrix phase and high purity. The change of growth rate with temperature through T_R and the temperature dependence of $\sigma(T)$ estimated from it were found to agree well with the theoretical predictions of the SOS model [41]. The change of curvature near T_R was also found to agree with the theoretical prediction [39]. The edges and corners of NaCl [42], Au [43, 44], and Pb [45, 46] crystals were observed to become curved at high temperatures, and flat low index surfaces of Ag_2S crystal were found to shrink until they became curved at their respective T_R [47]. The voids in some organic crystals were observed to change from polyhedral to spherical shapes with temperature increase [48–50].

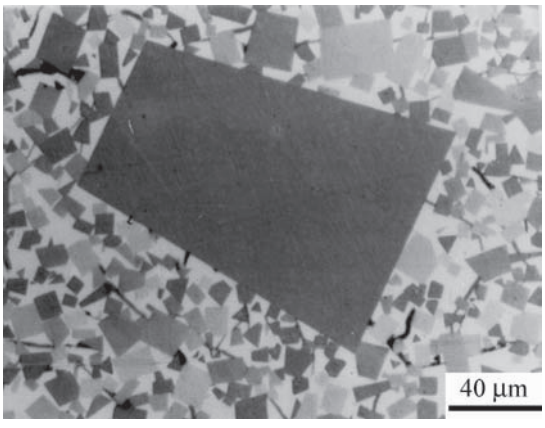

Figure 1 SEM micrograph of TaC-30wt%Ni alloy sintered at 1400°C for 8 h [57].

The theoretical analyses of the models for surfaces, which are the solid-vapor interfaces, are usually assumed to apply equally well to the solid-liquid interfaces. The crystal-melt interfaces in pure metals at the melting points are mostly rough. In many alloy systems, the approximate equilibrium shapes of grains in chemical equilibrium with liquid matrix can be observed in the specimens prepared, for example, by liquid phase sintering. Usually, the grains of compound phases show polyhedral shapes in the temperature ranges where liquid phases coexist as shown in Fig. 1 for TaC-30wt%Ni as an example, and metallic grains usually exhibit spherical shapes as shown in Fig. 2 for Mo-15wt%Ni. In many of these alloy systems, the temperature ranges for the solid-liquid coexistence are too limited to observe the roughening or the opposite singular transitions of the interfaces. But in NbC-transition metal, the grains in a transition metal-rich liquid matrix were observed to be polyhedral at low temperatures, curved at edges and corners at intermediate temperatures, and spherical at high temperatures [51–54]. Therefore, the roughening of the solid-liquid interface was found to qualitatively agree with the higher order transition predicted by the theoretical model. The addition of B to NbC-Fe [55] or NbC-Co [56] was also found to induce the roughening transition. The depletion of C in TaC-Ni was also found to induce the interface roughening [57].

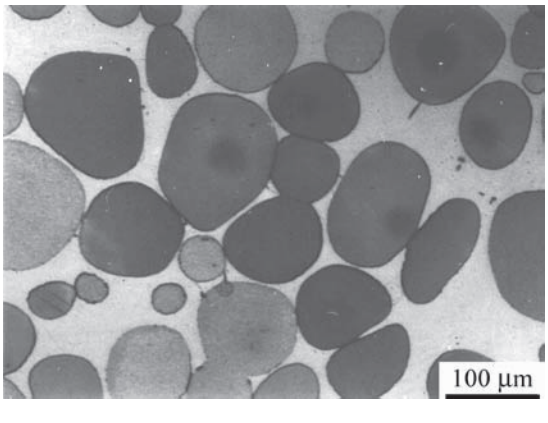

Figure 2 Optical micrograph of Mo-15wt%Ni alloy sintered at 1520°C for 20 h [103].

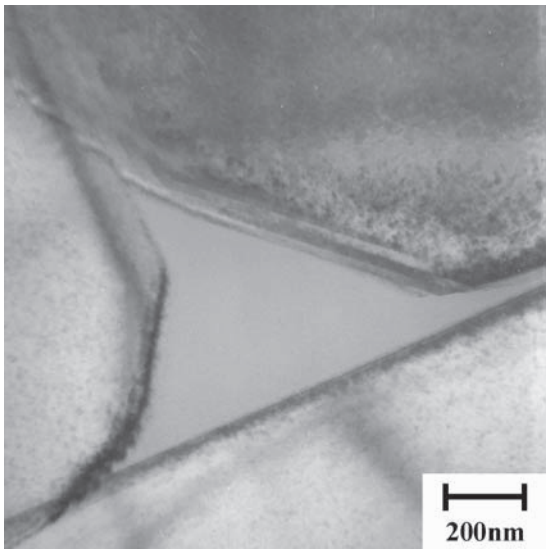

Figure 3 TEM micrograph of a triple junction of alumina-5wt% anorthite sintered at 1620°C for 48 h [104].

The roughening transitions of solid-solid heterophase interfaces were also reported for Ag-rich G.P. zones in Al-Ag alloy [58] and Ge particles in Al [59].

When alumina is sintered with small amounts of anorthite ($CaAl_2Si_2O_8$), which forms the liquid phase, the alumina grains in contact with liquid pockets at the grain triple junctions show faceted shapes with flat low index planes as shown in Fig. 3. These are singular interfaces. When MgO is added to the liquid phase, curved grain surfaces appear, although some flat surfaces still remain as shown in Fig. 4a. These curved surfaces must be rough, and their high resolution transmission electron microscope images (Fig. 4b) show the rough structure at atomic scale. Although the specimen was rapidly cooled from the sintering temperature, the interface structures as that shown in Fig. 4b will not accurately show those at high temperatures with possibly fluctuating surface steps. But at least the rapidly cooled structures like Fig. 4b confirm that there is no fine scale faceting or regular surface structure for these macroscopically curved surfaces. (There are cases when macroscopically curved surfaces actually consist of fine scale h&v structures which did not form during cooling. It is therefore necessary to confirm their singular or rough structures at atomic scales.)

Although the theoretical predictions of the SOS model agree with the observations in ideal systems like solid ^{4}He [38–41], it is presently not clear how well the SOS model with fluctuating lattice columns and voids of unlimited lengths can describe the roughening of various interfaces. It is possible that for solid-liquid or solid-solid interfaces, the two-dimensional Ising model with single atomic or molecular step height is more realistic. When the equilibrium shape of a crystal is spherical, the crystalline directionality is lost at the surface due to the dominant entropy effect. It thus appears to be clear that the surface becomes disordered at high temperature, although the roughening as described by various models may not accurately represent the phenomenon for all interface types. It has also been proposed [60–62] that surface premelting also occurs. But this is expected to occur at temperatures very close to the melting point and Beijeren and Nolden [7] concluded that the surface roughening was different from the premelting.

3. Roughening and defaceting transitions

The shape of a surface of an arbitrary average orientation schematically shown in the right column of Fig. 5 will depend on the crystal equilibrium shape shown in the left column of Fig. 5 at different temperatures. If the average orientation of a surface does not correspond to that which exists in the equilibrium, the surface will split into flat segments of h&v configuration as explained by Herring [1] and illustrated in Fig. 5a. If edges of the crystal at equilibrium become curved at a higher temperature and the surface slope changes discontinuously to the singular segment as illustrated in Fig. 5b, the arbitrary surface can still have an h&v shape with alternating singular and rough segments. As temperature increases further, the singular segment of the equilibrium shape will shrink, and in the h&v surface, the area of the rough segment will increase with its changing orientation. When the inflection point of the equilibrium shape moves so much to the center of

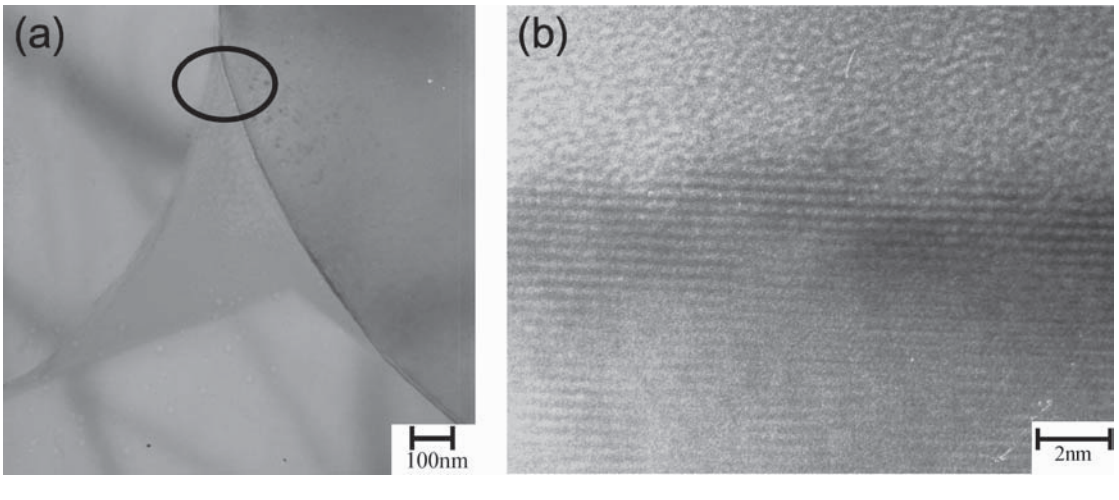

Figure 4 (a) TEM micrograph of a triple junction of alumina-5wt% anorthite sintered at 1620°C for 48 h and heat-treated again after packing in MgO powder for 6 h, and (b) high resolution TEM image of the boundary segment indicated by an ellipse in (a) [104].

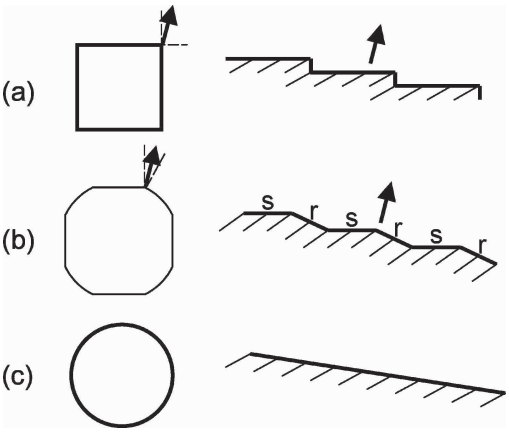

Figure 5 Schematic diagrams of equilibrium shapes (left column) and shapes of a surface segment with a fixed average orientation (right column) at (a) low, (b) intermediate, and (c) high temperatures.

the singular segment that the normal to the curved segment at the inflection point coincides with the average direction of the h&v surface, it will lose its h&v shape as the singular segments disappear and only the rough segments remain as illustrated in Fig. 5c. The defaceting transition thus occurs when a surface loses its h&v shape and becomes rough with a macroscopically curved shape because of its finite size. Because the defaceting transition of a surface of arbitrary orientation occurs as the roughening progresses in the equilibrium shape, it is usually a manifestation of the roughening transition. (Although the roughening transition always implies the defaceting transition, the latter does not always imply the former, because an h&v surface can entirely consist of rough segments. But an equilibrium shape with only rough surfaces meeting each other at sharp edges is very unlikely.)

The thermal faceting of polycrystalline metals with h&v structures is well known [63] as shown in Fig. 6 for an example. Because the equilibrium shapes of crystals at high temperatures usually consist of both singular and rough surfaces [42–47], some grain surfaces of a polycrystal will be rough with smoothly curved shapes while others have h&v shapes. If all singular surfaces in the equilibrium shape become rough, all grain surfaces of a polycrystal will also be rough with smoothly curved shapes.

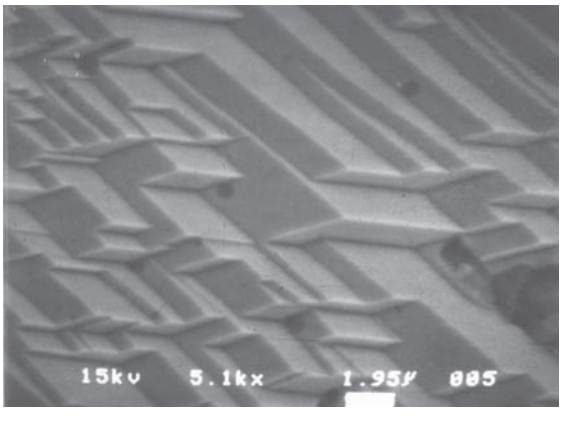

Figure 6 SEM micrograph of the hill-and-valley surface of a grain in an Ag polycrystal heat-treated at 800°C in an oxygen containing atmosphere [105].

4. Grain boundary roughening transition in oxides

In 1969 and 1970, Aust [29, 64] and Gleiter [65] made apparently the first suggestions that grain boundaries underwent phase transition, based on their analysis of grain growth kinetics and triple junction equilibria in Pb and its alloy. In 1970, Hart [66] also made the same suggestion and performed a thermodynamic analysis of this transition assuming it to be a first order transition [67].

It is possible that grain boundaries undergo continuous roughening transitions analogous to surfaces. Simple step models [68], SOS [36], and Ising models [69] predict that the roughening temperature T_R will be proportional to the step internal energy $\sigma(0)$. Since $\sigma(0)$ for a grain boundary will be lower than that for a surface, T_R of a grain boundary will be lower than that of a surface. Therefore, while surface roughening occurs at temperatures close to the bulk melting point T_m, the grain boundary roughening can occur at temperatures below T_m. Rottman [10] calculated the values of $\sigma(0)$ for low angle grain boundaries in Cu and predicted that the roughening should occur at temperatures below T_m for misorientation angles larger than a critical value.

Although the observations of grain boundary roughening transitions in oxides are less numerous than those in metals, their interpretations are more straightforward. Oxide ceramics are usually sintered with small amounts of liquid phases. But even in these ceramics some grain boundaries are not penetrated by the liquid phases and hence exist without any liquid layer. Some oxides can be almost fully sintered without any liquid phase and hence have only grain boundaries. Some of the grain boundaries in sintered oxides were observed to have either flat or h&v shapes. Some h&v grain boundaries consisted of several alternating boundary segments of the same orientations, while others showed only two boundary segments meeting at a single edge to form a kink as shown in Fig. 7 for an example. Grain boundaries with h&v shapes were observed in Mn-Zn ferrite [70], MgO [71, 72], and alumina [17, 18, 73–76].

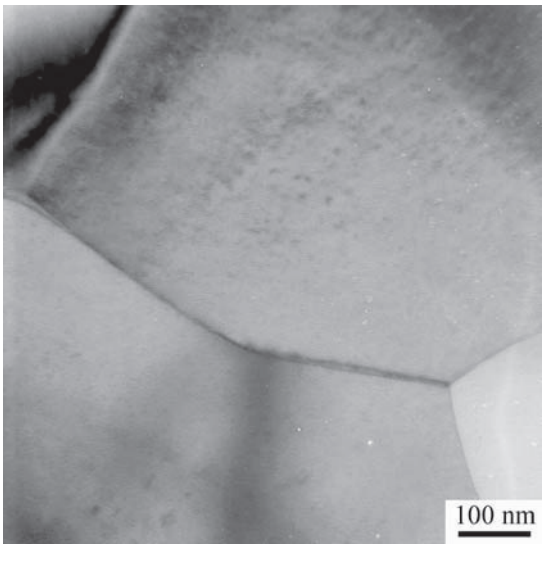

Figure 7 TEM micrograph of a kinked grain boundary in alumina sintered at 1400°C for 3 h and heat-treated at 1100°C for 24 h [106].

These flat grain boundaries and some segments of the h&v grain boundaries were observed to lie on low index planes of one of the grain pairs by TEM. In alumina doped with TiO_2, Y_2O_3, SiO_2, or CaO, flat grain boundaries lying on basal {0001}, rhombohedral {0112}, or other low index planes of one of the grain pairs were observed usually by HRTEM [17, 18, 75–77]. In a polycrystalline TiO_2-excess $BaTiO_3$, Yamamoto *et al.* [78, 79] and Lee *et al.* [23, 24] observed h&v grain boundaries with segments lying on {111} and {012} planes of one of the grains. Merkle and Smith [80] observed that ⟨100⟩ tilt grain boundaries in NiO had microfacets lying on {100} planes of one of the grains. These grain boundaries and segments lying on the low index planes of one of the grain pairs, which will be referred to as the low index grain boundaries, are likely to be singular, because they are flat and frequently appear as stable configurations.

The grain boundaries in high-purity alumina sintered at 1620°C were observed to be smoothly curved and hence rough. When this alumina was heat-treated again at 900, 1000, and 1100°C, some grain boundaries developed h&v shapes with the flat segments lying on a low index plane of one of the grain pairs as shown in Fig. 8. It is possible that the other grain boundaries remained rough because their roughening temperature was lower than 900°C. When these alumina specimens heat-treated at low temperatures were heat-treated again at 1620°C, all grain boundaries became defaceted. This reversible faceting-defaceting transition shows that the grain boundary roughening transition can be induced by temperature change in alumina.

The grain boundary roughening transition can also be induced by composition changes. When alumina doped with SiO_2 and CaO, and $BaTiO_3$ with excess TiO_2 are sintered in air, abnormal grain growth occurs [17, 18, 21–24], and the grain boundaries formed between the abnormal grains and the finer matrix grains are the most obvious examples of the singular grain boundaries. In alumina sintered with 100 ppm (by mole) of SiO_2 and 50 ppm of CaO at 1620°C, the abnormal grains are elongated along their basal planes as shown in Fig. 9a. The grain boundaries formed by these basal planes of the large grain and the small matrix grains are mostly straight across the triple junctions. Because the triple junctions were strongly etched thermally, deep grooves appear at the triple junctions in this SEM micrograph, but TEM micrographs confirmed that these basal grain boundaries were indeed straight across most of the triple junctions [18]. Such straight grain boundaries indicate that they behave like twin boundaries with strong torque effects and are possible if, and only if, they are singular as shown by the capillarity vector analysis [18]. Such straight grain boundaries were also observed between the matrix grains as indicated by

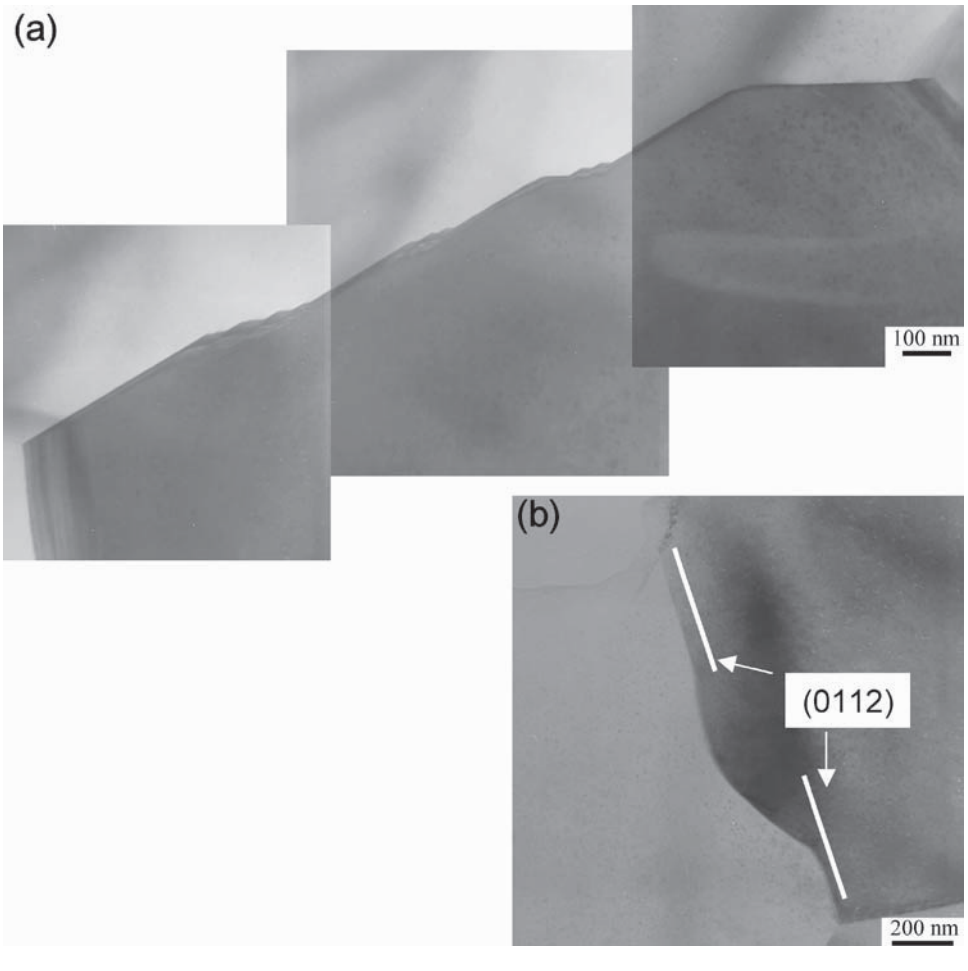

Figure 8 TEM micrographs of hill-and-valley grain boundaries in alumina (a) sintered at 1400°C for 24 h and heat-treated at 1000°C for 12 h, and (b) sintered at 1400°C for 3 h and heat-treated at 1000°C for 4 days [106].

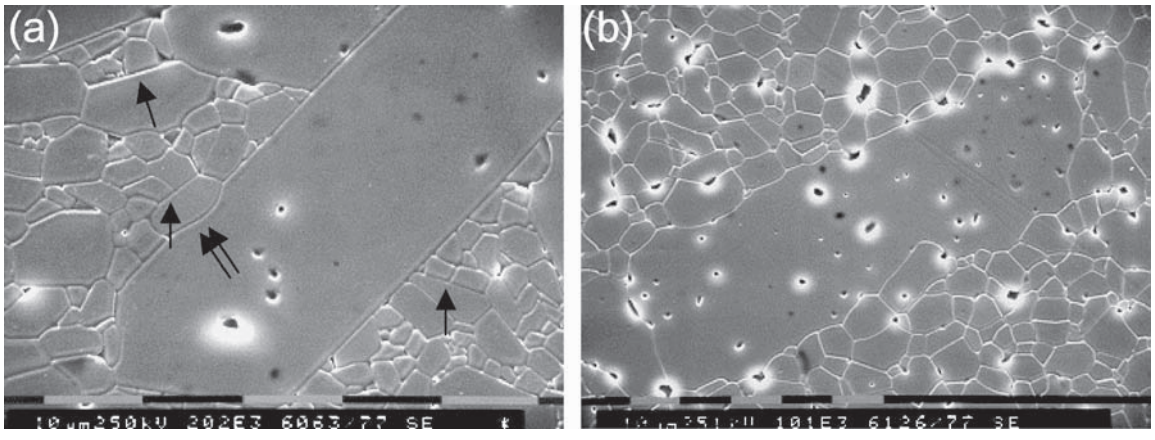

Figure 9 SEM micrographs of alumina doped with 100 mol ppm of SiO_2 and 50 mol ppm of CaO (a) sintered at 1620°C for 24 h, and (b) heat-treated again at 1620°C for 10 h after packing in MgO [107].

the single arrows in Fig. 9a. There were also curved grain boundaries between the large grain and the matrix grains as indicated by a double arrow in Fig. 9a, but TEM observations showed that these grain boundaries had h&v structures with boundary segments parallel to the basal plane. Such straight grain boundaries were also formed when a sapphire single crystal with basal surfaces was diffusion bonded to fine grains containing the same amounts of SiO_2 and CaO.

When the SiO_2-CaO doped specimen was heat-treated again at the same temperature after packing in MgO, the straight boundaries between the abnormal grain and the matrix grains and between the single crystal sapphire and the matrix grains became curved as shown in Fig. 9b. TEM observations showed [18] these grain boundaries to be curved even at high magnifications, indicating that they were rough. Therefore, the change of the straight basal grain boundaries shown in Fig. 9a to curved shapes shown in Fig. 9b represent the most direct observation of the grain boundary roughening transition.

When a sapphire crystal with basal planes was sintered with pure alumina powder, the grain boundaries between the single crystal and the fine matrix grains were curved and therefore rough. When this specimen was heat-treated again after packing in a powder containing 100 ppm of SiO_2 and 50 ppm of CaO, straight basal grain boundaries formed with shapes similar to those shown in Fig. 9a. This was a direct observation of the singular transition of the grain boundaries: the reverse of the roughening transition. The rough grain boundaries formed between the basal plane of the sapphire and the matrix grains can become flat upon heat-treating at low temperatures like 900, 1000, or 1100°C, but the kinetics was slow and the curved boundaries developed only kinked shapes [106].

Similar grain boundary roughening transition was observed in $BaTiO_3$ doped with 0.2 mol% TiO_2 [21]. When sintered in air at 1250°C, abnormal grain growth occurred with the abnormal grains elongated parallel to {111} double twins. The grain boundaries between the abnormal and the fine matrix grains were mostly straight across the triple junctions. When heat-treated in hydrogen at the same temperature, these straight grain boundaries became curved, showing their roughening transition. The high resolution TEM observations confirmed that the boundaries were either flat or curved even at atomic scales [23, 24]. The grain boundaries between the fine matrix grains had h&v structures when heat-treated in air and became defaceted (curved) in hydrogen, again indicating their roughening transition [21]. It was also reported that a $\sum 5$ grain boundary in $SrTiO_3$ showed defaceting transition with temperature increase [81].

In summary, the grain boundaries in pure alumina are rough at 1620°C and some become singular at temperatures between 900 and 1100°C. The addition of SiO_2-CaO induces singular transition and the addition of MgO induces roughening transition at 1620°C. The grain boundaries in TiO_2-excess $BaTiO_3$ are singular or rough in air or hydrogen, respectively, at 1250°C. The grain boundary roughening transition has not been investigated in other oxides or ceramics.

5. Grain boundary roughening transition in metals

In some metals, as in oxides, flat grain boundaries lying on certain crystallographic planes of either one or both grains were observed as reviewed by Wolf and Merkle [82]. For examples, Ichinose and Ishida [83] observed by HRTEM that about 30% of ⟨110⟩ tilt grain boundaries in a polycrystalline Au film lay on {111} planes of one of the grain pairs. They also observed that some grain boundaries in α-Fe lay on {200} planes of one of the grains. They called these low index crystal plane grain boundaries. For brevity, these were called low index grain boundaries for oxides in this report. Similar grain boundaries lying on {111} planes were also observed by Merkle and Wolf [84] in an Au ⟨110⟩ tilt bicrystal. Pennison [85] observed a high angle tilt grain boundary in Mo parallel to {110} plane of one grain and a high index plane of the other. The frequent observation of such low index grain boundaries indicates that they are the singular grain boundaries with the minimum boundary energies with respect to the variation of the inclination angle.

Both h&v and kinked grain boundaries were also observed in many metals for general and CSL misorientations in polycrystals and bicrystals. For the boundaries

with CSL misorientations, the flat segments of the h&v boundaries were sometimes observed to lie on the planes of high CSL density, but for those with general misorientation angles, the planes of the h&v segments were not usually determined. The existence of the h&v grain boundaries indicates that for the grain boundaries with any misorientation angle, the boundary energy varies with the orientation of the boundary plane (the inclination angle) and the some flat segments correspond to the singular orientations. But it is also possible that some flat segments of the h&v boundaries are rough if the grain boundary Wulff shape (of an island grain embedded in a larger grain) has curved segments with slope discontinuities.

Some grain boundaries were observed to have kinks [86–89], where the boundary plane orientation changed discontinuously. These appeared frequently at the boundaries with sharply curved overall shapes as in the reverse capillarity bicrystals [88, 89]. Such kinks are also called shocks. Because these kinks are likely to correspond to the edges and corners in the grain boundary Wullf shapes, one or both boundary planes on either side of them are likely to be singular. Therefore, the kinked boundaries can be regarded as special cases of h&v boundaries.

When heat-treated at high temperatures, the h&v grain boundaries in some metals were observed to become defaceted with smoothly curved shapes. Such a defaceting transition of grain boundaries was first reported by Henry *et al.* [14] in bulk polycrystalline Ni. When slowly cooled after heat-treating at 1050°C, the grain boundaries showed h&v shapes, but when quenched in water, they were smoothly curved. When heat-treated at 650°C, the intergranular fracture surfaces showed distinct h&v shapes, and the tendency to form h&v grain boundaries was enhanced by oxygen in the heat-treatment atmosphere.

The first definitive observations of faceting-defaceting grain boundary transitions were observed by Hsieh and Balluffi [11] for $\Sigma = 3$ asymmetric $\langle 111 \rangle$ tilt boundaries in Al and Au, and for $\Sigma = 11$ asymmetric $\langle 110 \rangle$ tilt boundary in Au. The *in-situ* TEM observations showed h&v boundaries at low temperatures becoming defaceted at temperatures above 0.54 T_m and regaining the h&v shapes at low temperatures. Westmacott and Dahmen [90] also observed that a nearly polyhedral island grain of Al with $\Sigma = 99$ $\langle 110 \rangle$ tilt boundaries developed curved edges upon heating to 430°C (0.75 T_m) and became again polyhedral upon cooling. This was the first direct observation of the grain boundary roughening transition.

The first observations of defaceting transitions of general grain boundaries in polycrystals were recently made in Ni [15], Ag [16], Cu [93, 94], 316L stainless steel [91, 92], a Ni-base superalloy [95, 96], and a Si-iron alloy [97]. When heat-treated at relatively low temperatures, many grain boundaries showed h&v or kinked shapes, and when heat-treated at temperatures close to T_m, all grain boundaries (except those in Cu) became defaceted. In Ni [15] and Ag [16], the defaceting transitions were shown to depend on the atmosphere used for the heat-treatment. Fig. 10a shows, as an example, an h&v grain boundary in 316L stainless heat-treated at 1100°C. When heat-treated at 1300°C, all grain boundaries became defaceted with curved shapes as shown in Fig. 10b. In these polycrystalline specimens, the observations of the defaceting transitions were not made for the same grain boundaries, but the statistical analysis of the fractions of the randomly selected h&v and defaceted grain boundaries at different heat-treatment temperatures clearly showed that the general grain boundaries underwent defaceting transitions at temperatures above about 0.7 T_m.

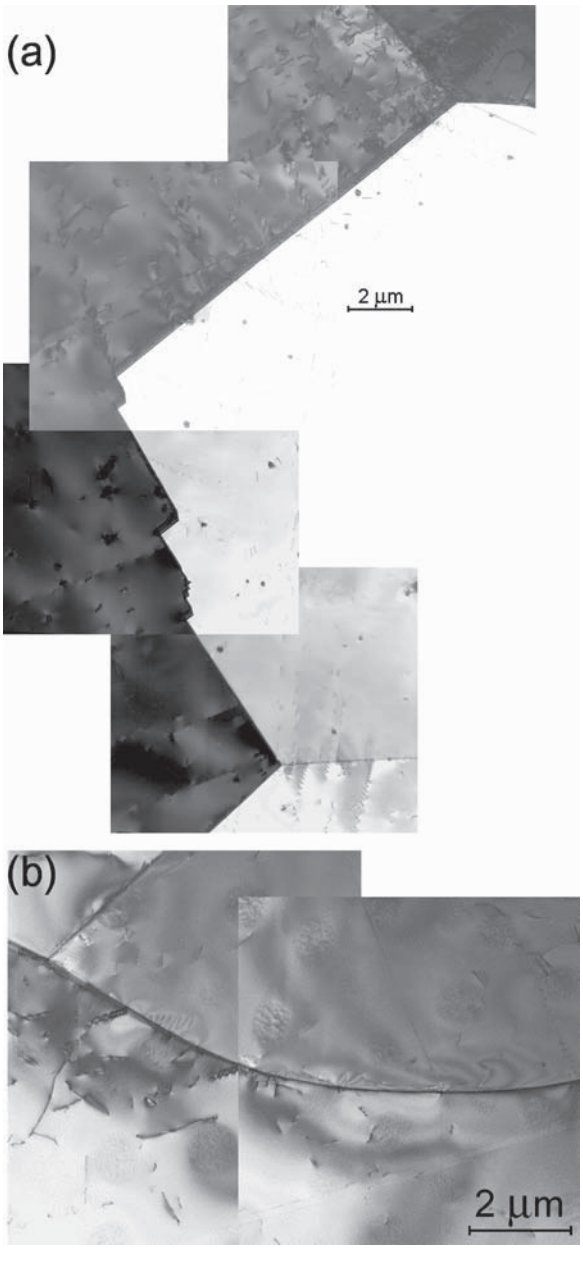

Figure 10 TEM micrographs of grain boundaries in 316L stainless steel heat-treated (a) at 1100°C for 1 h and (b) at 1300°C for 15 min [108].

As in oxides, the addition of solute species was also observed to induce the development of h&v structures. The grain boundaries in Cu and α-Fe developed h&v shapes when Bi [12, 99–102] and Te [13, 98] were respectively added. When Bi was removed from Cu-Bi alloy, the grain boundaries became defaceted [12]. These additive effects are similar to those observed in alumina

and $BaTiO_3$ described earlier in this report. Presently, it is not understood why these additives produce such singular or roughening transitions.

6. Heat-treatment of grain boundaries

It now appears that the grain boundaries in all metals examined so far undergo roughening transitions at temperatures above about 0.7 T_m. The twin boundaries and some grain boundaries may remain singular even at the melting point. The grain boundary roughening transition may have important implications for obtaining the grain boundaries with desired structures and properties.

If a grain boundary is rough, its structure and properties will be nearly isotropic with respect to both the misorientation angle between the grains and the boundary plane. Therefore, if all grain boundaries in a polycrystal are rough, they will have nearly uniform structures and properties. The high resolution TEM observations of the rough grain boundaries in the specimens that were quenched from high temperatures show that the rough boundary structures or at least their locations can be largely retained during cooling without developing any fine scale h&v or kinked structures. This means that the faceting transition, which usually occurs by nucleation and growth process, may be sufficiently slow during cooling.

On the other hand, if the heat-treatment temperature is below the roughening transition temperatures of most of the boundaries, the grain boundaries will develop flat segments, h&v shapes, and kinks to produce singular structures corresponding to the cusps in the polar plot (the Wulff plot) of the grain boundary energy against the inclination angle. It is thus possible to produce either quenched rough or singular grain boundaries by simply heat-treating the grain boundaries in both metals and oxides at temperatures above or below T_R for most of the grain boundaries. It is expected that many grain boundary properties and processes such as corrosion, fracture, diffusion, sliding, and precipitation will depend on this structural transformation. The electrical properties related to grain boundaries in oxides may also depend on this structural transformation. It should be noted that the grain boundary heat-treatment based on the roughening transition does not require any changes of the orientations of the grains. Even for a polycrystal with fixed grain orientations, the grain boundaries can become either rough or singular by their relatively slight movements during the heat-treatment.

In metals and oxides, it was shown that the grain growth behavior was closely correlated to the grain boundary roughening transition [15, 16, 21, 22, 91–97]. When most of the grain boundaries were either flat, h&v type, or kinked at low temperatures or with additives, abnormal grain growth occurred, and when all grain boundaries were curved and hence rough, normal grain growth occurred. The abnormal grain growth was attributed to the step migration mechanism of the singular boundaries. Therefore, the polycrystals that showed abnormal grain growth will have mostly singular grain boundaries while those that showed normal growth will have rough grain boundaries with corresponding different grain boundary properties in addition to the differences in grain size. At certain temperatures, both faceted and curved grain boundaries can coexist, as shown in Fig. 11, because of different T_R for each grain boundary. It is expected that in such a case, the properties are expected to vary from the singular to rough boundaries, and the migration of the intersecting grain boundaries including that of the triple junction will critically depend on temperature because of the boundary transformations. The dihedral angles between the grain boundaries intersecting at a triple point will also change when they undergo roughening-singular transitions. As shown in Fig. 7, a singular segment often intersects another segment with a kink, which cannot be often detected by casual observation.

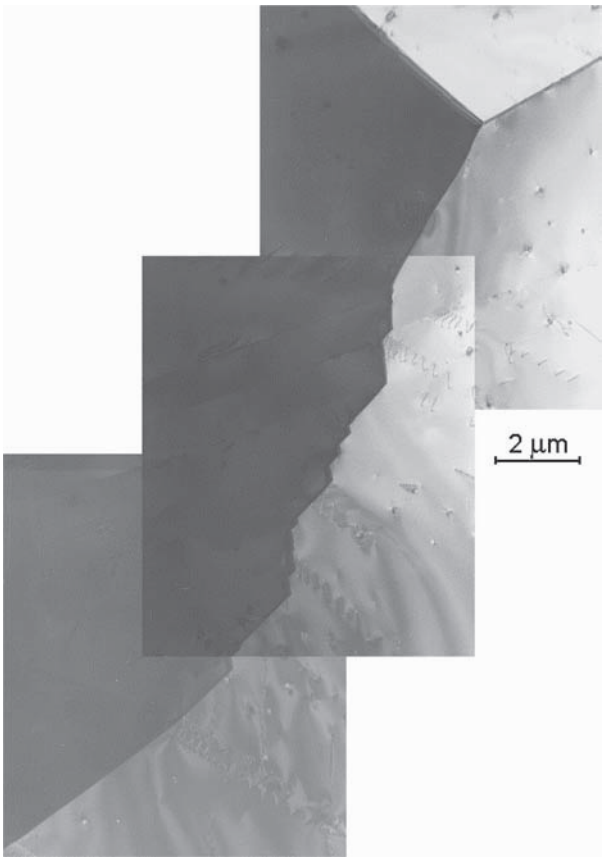

Figure 11 TEM micrograph of a faceted grain boundary intersecting two curved (rough) grain boundaries at a triple junction in 316L stainless steel heat-treated at 1100°C for 1 h [108].

7. Conclusions

In the processing of bulk polycrystalline materials, it may not be easy to control the grain orientations to improve the properties related to grain boundaries. The grain boundary roughening transition presents the possibility of altering the grain boundary properties by heat-treatment or additives without changing the grain orientations. It is possible that such low temperature properties as corrosion and fracture depend on the quenched rough or singular boundary structures. The temperature dependent properties such as superplasticity and sintering may also depend on the grain boundary structural transformation.

Acknowledgement

One of the authors (D. Y. Yoon) is grateful to Korea Electronic Power Corporation for the chair-professorship, which supported a part of this work.

References

1. C. HERRING, *Phys. Rev.* **82** (1951) 87.
2. W. K. BURTON and N. CABRERA, *Dis. Faraday Soc.* **5** (1949) 33.
3. W. K. BURTON, N. CABRERA and F. C. FRANK, *Phil. Trans. R. Soc. London Sect. A* **243** (1951) 299.
4. F. C. FRANK, in "Metal Surfaces: Structure, Energetics, and Kinetics", edited by W. D. Robertson and N. A. Gjostein (American Society for Metals, Metals Park, OH, 1963) p. 1.
5. J. D. WEEKS and G. H. GILMER, in "Advances in Chemical Physics", edited by I. Prigogine and S. A. Rice (Wiley, NY, 1979) Vol. 40, p. 157.
6. J. D. WEEKS, in "Ordering in Strongly Fluctuating Condensed Matter Systems", edited by T. Riste (Plenum, New York, 1980) p. 293.
7. H. VAN BEIJEREN and I. NOLDEN, in "Structure and Dynamics of Surfaces II: Phenomena, Models, and Method", edited by W. Schommers and P. von Blanckenhagen (Springer-Verlag, Berlin, 1987) p. 259.
8. M. WORTIS, in "Chemistry and Physics of Solid Surfaces VII", edited by R. Banselow and R. F. Howe (Springer-Verlag, Berlin, 1987) p. 367.
9. E. H. CONRAD, *Prog. Surf. Sci.* **39** (1992) 65.
10. C. ROTTMAN, *Phy. Rev. Lett.* **57** (1986) 735.
11. T. E. HSIEH and R. W. BALLUFFI, *Acta Metall.* **37** (1989) 2133.
12. T. G. FERENCE and R. W. BALLUFFI, *Scripta Metall.* **22** (1988) 1929.
13. J. R. RELLICK, C. J. MCMAHON JR., H. L. MARCUS, and P. W. PALMBERG, *Metall. Trans.* **2** (1971) 1492.
14. G. HENRY, J. PLATEAU, X. WACHE, M. GERBER, I. BEHAR and C. CRUSSARD, *Mem. Sci. Rev. Metall.* **56** (1959) 417.
15. S. B. LEE, N. M. HWANG, D. Y. YOON and M. F. HENRY, *Metall. Mater. Trans. A* **31** (2000) 985.
16. J. B. KOO and D. Y. YOON, *ibid.* **32** (2001) 469.
17. C. W. PARK and D. Y. YOON, *J. Am. Ceram. Soc.* **83** (2000) 2605.
18. C. W. PARK, D. Y. YOON, J. E. BLENDELL and C. A. HANDWERKER, *ibid.* **83** (2003) 603.
19. T. YAMAMOTO, *British Ceram. Trans.* **94** (1995) 196.
20. T. YAMAMOTO and T. SAKUMA, *Mater. Sci. Forum* **204–206** (1996) 491.
21. B.-K. LEE, S.-Y. CHUNG and S.-J. L. KANG, *Acta Mater.* **48** (2000) 1575.
22. Y. K. CHO, S.-J. L. KANG and D. Y. YOON, *J. Am. Ceram. Soc.* submitted for publication.
23. S. B. LEE, S.-Y. CHOI and D. Y. YOON, *Z. Metallkd.* **94** (2003) 193.
24. S. B. LEE, W. SIGLE and M. RÜHLE, *Acta Mater.* **50** (2002) 2151.
25. L. S. SHVINDLERMAN and B. B. STRAUMAL, *Acta Metall* **33** (1985) 1735.
26. T. WATANABE, S.-I. KIMURA and S. KARASHIMA, *Phil. Mag. A* **49** (1984) 845.
27. P. LAGARDE and M. BISCONDI, *Mém. Sci. Rev. Métall.* **71** (1974) 121.
28. *Idem.*, *Can. Metall. Quart.* **13** (1974) 245.
29. K. T. AUST, in "Interfaces Conference, Melbourne", edited by R. C. Gifkins (The Australian Institute of Metals, Butterworth, London, 1969) p. 307.
30. S. T. TSUREKAWA and H. NAKASHIMA, *Mater. Sci. Forum* **204–206** (1996) 221.
31. S. T. TSUREKAWA, T. UEDA, K. ICHIKAWA, H. NAKASHIMA, Y. YOSHITOMI and H. YOSHINAGA, *Mater. Sci. Forum* **294–296** (1999) 629.
32. L. ONSAGER, *Phys. Rev.* **65** (1944) 117.
33. S. T. CHUI and J. K. WEEKS, *Phys. Rev. B* **14** (1972) 4978.
34. J. M. KOSTERLITZ and D. J. THOULESS, *J. Phys. C* **6** (1973) 1181.
35. H. J. LEAMY and G. H. GILMER, *J. Cryst. Growth* **24/25** (1974) 499.
36. H. VAN BEIJEREN, *Phys. Rev. Lett.* **38** (1977) 993.
37. C. ROTTMAN and M. WORTIS, *Phys. Rep.* **103** (1984) 59.
38. J. E. AVRON, L. S. BALFOUR, C. G. KUPER, J. LANDAU, S. G. LIPSON and L. S. SCHULMAN, *Phys. Rev. Lett.* **45** (1980) 814.
39. S. BALIBAR and B. CASTAING, *J. Physique Lett.* **41** (1980) L-32.
40. K. O. KESHISHEV, A. Y. PARSHIN and A. V. BABKIN, *Zh. Eksp. Teor. Fiz.* **80** (1981) 716. (*Sov. Phys. JETP* **53** (1981) 362).
41. P. E. WOLF, F. GALLET, S. BALIBAR, E. ROLLEY and P. NOZIÈRES, *J. Physique* **46** (1985) 1987.
42. J. C. HEYRAUD and J. J. MÈTOIS, *J. Cryst. Growth* **84** (1987) 503.
43. *Idem.*, *ibid.* **50** (1980) 571.
44. *Idem.*, *Acta Metall.* **28** (1980) 1789.
45. *Idem.*, *Surf. Sci.* **128** (1983) 334.
46. C. ROTTMAN, M. WORTIS, J. C. HEYRAUD and J. J. MÈTOIS, *Phys. Rev. Lett.* **52** (1984) 1009.
47. T. OHACHI and I. TANIGUCHI, *J. Cryst. Grwoth* **65** (1983) 84.
48. PAVLOVSKA and D. NENOW, *Surf. Sci.* **27** (1971) 211.
49. *Idem.*, *J. Cryst. Growth* **12** (1972) 9.
50. *Idem.*, *ibid.* **39** (1977) 346.
51. S. SARIAN and H. W. WEART, *Trans. Metall. Soc. AIME* **233** (1965) 1990.
52. R. WARREN, *J. Mater. Sci.* **3** (1968) 471.
53. *Idem.*, *J. Less-Common Metals* **17** (1969) 65.
54. Y. K. CHO and D. Y. YOON, *J. Am. Ceram. Soc.* submitted for publication.
55. K.-S. OH, J.-Y. JUN and D.-Y. KIM, *ibid.* **83** (2000) 3117.
56. H. S. MOON, B.-K. KIM and S.-J. L. KANG, *Acta Mater.* **49** (2001) 1293.
57. J. H. CHOI, "Effect of Carbon on the Grain Growth Behavior in TaC-Ni", (M.S. Thesis, KAIST, Korea, 1997).
58. K. B. ALEXANDER, F. K. LEGOUES, H. I. AARONSON and D. E. LAUGHLIN, *Acta Metall.* **32** (1984) 2241.
59. P. LOURS, K. H. WESTMACOTT and U. DAHMEN, in "Structure and Properties of Interfaces in Materials, Materials Research Society Symposium Proceedings", edited by W. A. T. Clark, U. Dahmen and C. L. Briant (Materials Research Society, Pittsburgh, PA, 1992) Vol. 238, p. 207.
60. D. NENOW, *Prog. Cryst. Growth and Charact.* **9** (1984) 185.
61. J. W. M. FRENKEN and J. F. VAN DER VEEN, *Phys. Rev. Lett.* **54** (1985) 134.
62. J. Q. BROUGHTON and G. H. GILMER, *J. Phys. Chem.* **91** (1987) 6347.
63. A. J. W. MOORE, in "Metal Surfaces: Structure, Energetics and Kinetics", edited by W. D. Robertson and N. A. Gjostein (American Society for Metals, Metals Park, Ohio, 1963) p. 155.
64. K. T. AUST, *Canadian Metallurgical Quarterly* **8** (1969) 173.
65. H. GLEITER, *Z. Metallkde* **61** (1970) 283.
66. E. W. HART, in "Ultrafine Grain Metals", edited by J. J. Burke, N. L. Reed and V. Weiss (Syracuse University Press, Syracuse, NY, 1970) p. 247.
67. E. W. HART, in "The Nature and Behaviour of Grain Boundaries", edited by H. Hu (Plenum Press, NY, 1972) p. 155.
68. Y. SAITO, in "Statistical Physics of Crystal Growth" (World Scientific, Singapore, New Jersey, London, Hong Kong, 1996) p. 1.
69. E. BURKNER and D. STAUFFER, *Z. Phys. B* **53** (1983) 241.
70. M. L. GIMPL, A. D. MCMASTER and N. FUSCHILLO, in "Materials Science Research", edited by W.W. Kriegel and H. Palmour III (Plenum Press, New York, 1966) Vol. 3, p. 183.
71. N. J. TIGHE and J. R. KREGLO, JR., *Ceramic Bulletin* **49** (1970) 188.
72. N. J. TIGHE, in "Ultrafine-Grain Ceramics", edited by J. J. Burke, N. L. Reed and V. Weiss (Syracuse University Press, Syracuse, NY, 1970) p. 109.

73. N. J. TIGHE and J. R. KREGLO, *Am. Ceram. Soc. Bull.* **49** (1970) 188.
74. K. J. MORRISSEY and C. B. CARTER, *J. Am. Ceram. Soc.* **67** (1984) 292.
75. D. W. SUSNITZKY and C. B. CARTER, *ibid.* **73** (1990) 2485.
76. M. A. GÜLGÜN, V. PUTLAYEV and M. RÜHLE, *ibid.* **82** (1999) 1849.
77. S. LARTIGUE, L. PRIESTER, F. DUPAU, P. GRUFFEL and C. CARRY, *Mater. Sci. Eng. A* **164** (1993) 211.
78. T. YAMAMOTO, Y. IKUHARA, K. HAYASHI and T. SAKUMA, *J. Mater. Res.* **13** (1998) 3449.
79. T. YAMAMOTO, Y. IKUHARA, K. HAYASHI and T. SAKUMA, *Mater. Sci. Forum* **294–296** (1999) 247.
80. K. L. MERKLE, *Ultramicroscopy* **22** (1987) 57.
81. S. B. LEE, W. SIGLE, W. KURTZ and M. RÜHLE, *Acta Mater.* **51** (2003) 975.
82. D. WOLF and K. L. MERKLE, in "Materials Interfaces: Atomic-level Structures and Properties", edited by D. Wolf and S. Yip (Chapman & Hall, London, 1992) p. 87.
83. H. ICHINOSE and Y. ISHIDA, *J. de Physique* **46 C4**(suppl.) (1985) 39.
84. K. L. MERKLE and D. WOLF, *Phil. Mag. A* **65** (1992) 513.
85. J.-M. PENISSON, *J. de Physique* **49 C5**(suppl.) (1988) 87.
86. M. J. WEINS and J. J. WEINS, *Phil. Mag.* **26** (1972) 885.
87. A. I. BARG, E. RABKIN and W. GUST, *Acta Metall. Mater.* **43** (1995) 4067.
88. M. S. MASTELLER and C. L. BAUER, *Acta Metall.* **27** (1979) 483.
89. *Idem.*, *Phil. Mag. A* **38** (1978) 697.
90. K. H. WESTMACOTT and D. DAHMEN, in "Interface: Structure and Properties", edited by S. Ranganathan, C. S. Pande, B. B. Rath and D. A. Smith (Trans Tech Publications, Switzerland, 1993) p. 133.
91. J. S. CHOI and D. Y. YOON, *ISIJ International* **41** (2001) 478.
92. S.-H. LEE, J. S. CHOI and D. Y. YOON, *Z. Metallkd.* **92** (2001) 655.
93. J. B. KOO and D. Y. YOON, *Metall. Mater. Trans. A* **32** (2001) 1911.
94. J. B. KOO, D. Y. YOON and M. F. HENRY, *Metall. Mater. Trans. A* **33** (2002) 3803.
95. S. B. LEE, D. Y. YOON and M. F. HENRY, *Acta Mater.* **48** (2000) 3071.
96. Y. K. CHO, D. Y. YOON and M. F. HENRY, *Metall. Mater. Trans.* A **32** (2001) 3077.
97. J. S. CHOI and D. Y. YOON, *ISIJ International* **43** (2003) 245.
98. C. PICHARD, J. RIEU and C. GOUX, *Mémoires Scientifiques Rev. Métallurg*, **LXX** (1973) 13.
99. M. MENYHARD, B. BLUM, C. J. MCMAHON, JR. , S. CHIKWAMBANI and J. WEERTMAN, *J. de Physique* **49 C5** (suppl.) (1988) 457.
100. M. DONALD and L. M. BROWN, *Acta Metall.* **27** (1979) 59.
101. M. MENYHARD, B. BLUM and C. J. MCMAHON, JR., *ibid.* **37** (1989) 549.
102. E. C. URDANETA, D. E. LUZZI and C. J. MCMAHON, JR., *Mat. Res. Soc. Symp. Proc.* **238** (1992) 201.
103. W.-H. RHEE, The Interface Migration and Instability Induced by Diffusional Coherency Strain in Mo-Ni Alloy, Ph.D. Thesis, KAIST, Korea, 1988.
104. M. J. KIM, Effect of MgO Addition on Interface Structure and Grain Growth in Alumina-Anorthite, M. S. Thesis, KAIST, Korea, 2001.
105. J. B. KOO, unpublished work.
106. M. J. KIM, unpublished work.
107. C. W. PARK, unpublished work.
108. J. S. CHOI, "Effect of Grain Boundary Structure on Grain Growth Behavior in 316L Stainless Steel," M. S. Thesis, KAIST, Korea, 1997.